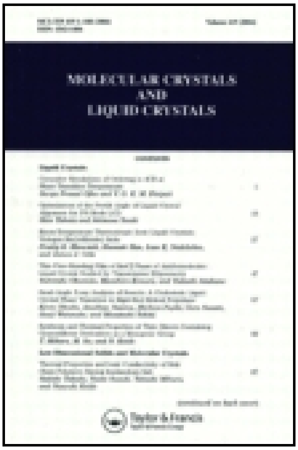

Molecular Crystals and Liquid Crystals

Publication details, including instructions for authors and subscription information:
http://www.tandfonline.com/loi/gmcl16

A Family of Ferroelectric Liquid Crystals with Very High Spontaneous Polarization

K. Mohr [a], S. Köhler [a], K. Worm [a], G. Pelzl [a], S. Diele [a], H. Zaschke [a], D. Demus [a], G. Andersson [b], I. Dahl [b], S. T. Lagerwall [b], K. Skarp [b] & B. Stebler [b]

[a] Chemistry Department, University of Halle, Halle (Saale), DDR

[b] Physics Department, Chalmers University of Technology, S-412 96, Göteborg, Sweden

To cite this article: K. Mohr , S. Köhler , K. Worm , G. Pelzl , S. Diele , H. Zaschke , D. Demus , G. Andersson , I. Dahl , S. T. Lagerwall , K. Skarp & B. Stebler (1987): A Family of Ferroelectric Liquid Crystals with Very High Spontaneous Polarization, Molecular Crystals and Liquid Crystals, 146:1, 151-171

To link to this article: http://dx.doi.org/10.1080/00268948708071811

Mol. Cryst. Liq. Cryst., 1987, Vol. 146, pp. 151–171
Photocopying permitted by license only

Printed in the United States of America

A Family of Ferroelectric Liquid Crystals with Very High Spontaneous Polarization

K. MOHR, S. KÖHLER, K. WORM, G. PELZL, S. DIELE, H. ZASCHKE and D. DEMUS

Chemistry Department, University of Halle, Halle (Saale), DDR

and

G. ANDERSSON, I. DAHL, S. T. LAGERWALL, K. SKARP and B. STEBLER

Physics Department, Chalmers University of Technology, S-412 96 Göteborg, Sweden

(*Received October 23, 1986*)

A new family of ferroelectric liquid crystals is presented. In particular, some mixtures of compounds from this family show an interesting combination of high spontaneous polarization, good alignment properties and room temperature smectic C* phase. Measurements are presented for transition enthalpies, refractive indices, X-ray tilt angle, electro-optic tilt angle and spontaneous polarization. The electro-optic response is described as measured in 2 micron thick shear-aligned cells.

INTRODUCTION

In the search for better ferroelectric smectic C* materials, we present here some families of new compounds characterized by a general structure similar to (i) and (ii) from Figure 1 or related compounds with cyclohexane or pyrimidine variations. The compounds are synthesized from amino-acids with valine, leucine and isoleucine as starting products and show a fast electro-optic response with polarization values slightly below 100 nC cm^{-2}. Whereas (ii) with $n = 12$ has a high-lying C* phase, from 81° to 159° Celcius, (i) with $n = 12$ has a

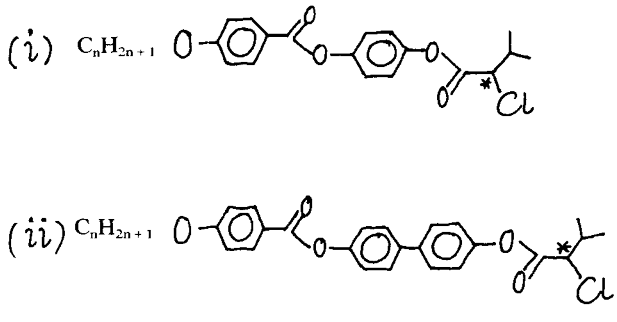

FIGURE 1 General structure formulae for the studied compounds.

low-lying but only monotropic C* phase. In Figures 2 and 3 we present however two typical binary and ternary mixtures showing the usefulness of the compounds. Electro-optic measurements will be presented below for these mixtures showing response times of the order of 10 μs at 10 volts/μm of applied field.

SYNTHESES OF THE COMPOUNDS

The syntheses followed the general scheme given below. Chiral amino acids 1 (L–(+) – valine, L–(+) – leucine, L–(+) – isoleucine) are transformed to the corresponding (*S*) – 2 – chloro – alkanoic acids 2 according to the instruction of Karrer *et al.*,[1] which are treated with thionylchloride to give the (*S*) – 2 – chloro – alkanoic acid chlorides 3.

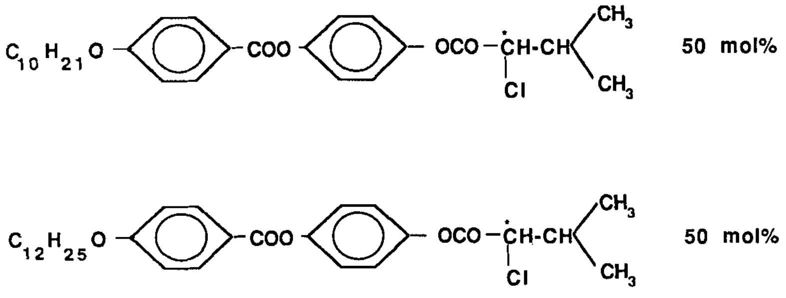

Cry 29 SmC* 43.5 SmA 70 N* 71 Iso

FIGURE 2 Typical low-melting binary mixture.

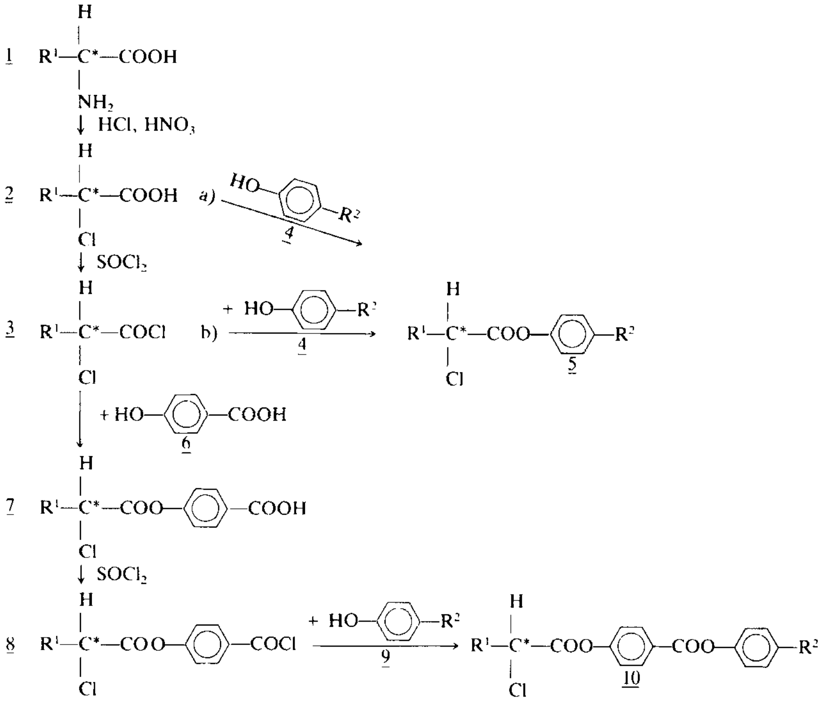

a) To obtain compounds 5 the acids 2 react with 4-substituted phenols 4 according to the following instruction: To 50 cm³ ether are added 0.01 mole acid 2, 0.01 mole dicyclohexylcarbodiimide, 0.001 mole 4-dimethylamino-pyridine and 0.01 mole substituted phenol 4. The mixture is allowed to stay 2 to 3 days at room temperature and the precipitation of N,N'-dicyclohexyl-urea is removed. The solution is washed several times with water, dried with sodium sulfate, the solvent is evaporated and the residue is recrystallized several times from methanol. The yields are 40 to 50% of those theoretically expected.

b) The compounds 5 may also be obtained by reaction of the acid chlorides 3 with the 4-subst. phenols 4:

To a solution of 0.005 mole 4-subst.phenol 4 in 0.6 cm³ triethylamine and 50 cm³ absolute toluene is added 0.005 mole acid chloride 3. The mixture is allowed to stay one day at ambient temperature and after this for one hour heated to 80°C on a water bath. After removal of the precipitation the solvent is evaporated and the residue is recrystallized from ethanol/water several times. The yields of 5 are 50 to 60% of the theoretical one.

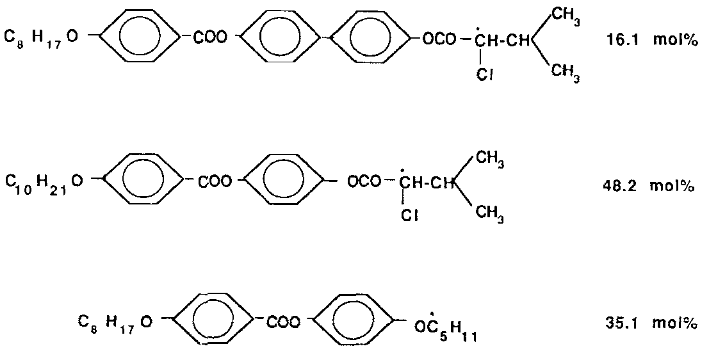

Cry 18 SmC* 45 SmA 74 N* 85 Iso

FIGURE 3 Ternary mixture.

Instead of 4 also 4-hydroxy benzoic acid 6 may react with 3 to give 7, which are converted by thionylchloride into the acid chlorides 8. The acid chlorides 8 may react with 4-subst. phenols 9 to the compounds 10 using the same instruction which was taken for the synthesis of 5.

The following Tables I–XIII present examples of the new compounds. Due to difficulties in the estrification, several compounds

TABLE I

(S)-4-(2-chloro-3-methyl-butanoyloxy)-4′-(4-subst.-benzoyloxy)-biphenyl

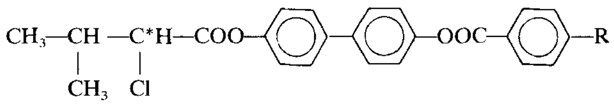

No.	R	Cr		G		C*		A		N*		is
1/1	$—OC_3H_7$	.	113	—	—	.	115	—	—	.	210	.
1/2	$—OC_4H_9$	.	106	—	—	.	126	—	—	.	211	.
1/3	$—OC_5H_{11}$	.	75	—	—	.	120	—	—	.	198	.
1/4	$—OC_6H_{13}$	.	85	—	—	.	132	—	—	.	195	.
1/5	$—OC_7H_{15}$	.	90	—	—	.	140	—	—	.	185	.
1/6	$—OC_8H_{17}$	.	87	—	—	.	154	—	—	.	188	.
1/7	$—OC_9H_{19}$	.	82	—	—	.	152	—	—	.	177	.
1/8	$—OC_{10}H_{21}$	.	80	—	—	.	155	—	—	.	172	.
1/9	$—OC_{12}H_{25}$	.	78	—	—	.	162	.	164	.	175	.
1/10	$—C_6H_{13}$	.	88	.	93	.	140	—	—	.	172	.
1/11	—CN	.	125	—	—	—	—	.	173	.	229	.
1/12	$—OCH_2—CH{=}CH_2$	.	97	—	—	.	104	—	—	.	207	.

TABLE II

(S)-4-(2-chloro-3-methyl-butanoyloxy)-4′(4-n-alkyl-cyclohexanoyloxy)-biphenyls

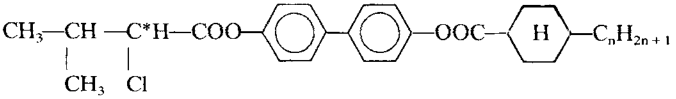

No.	n	Cr		B		A		N*		is
2/1	5	.	100	.	150	.	188	.	215	.
2/2	6	.	95	.	151	.	181	.	188	.
2/3	12	.	80	.	149	.	173	—	—	.

TABLE III

S-4-(2-chloro-3-methyl-butanoyloxy)-4′-subst.-biphenyls

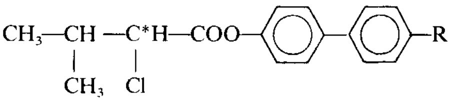

No.	R	Cr		C*		N*		is
3/1	—H	.	120	—	—	—	—	.
3/2	—COOH	.	222	.	240	.	260	.
3/3	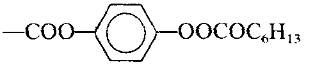	.	130	.	150	.	212	.
3/4	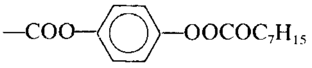	.	106	.	150	.	230	.

TABLE IV

(S)-1-(2-chloro-3-methyl-butanoyloxy)-4-(4-subst.-benzoyloxy)-benzenes

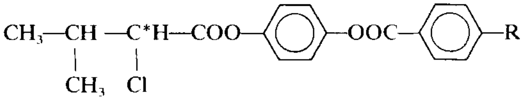

R	Cr		C*		A	N*		BP		is
$—OC_5H_{11}$	.	93	—	—	(. 64)	—	—	—	—	.
$—OC_6H_{13}$	.	88	—	—	(. 58)	—	—	—	—	.
$—OC_7H_{15}$	.	75	—	—	(. 54	.	56	.	58)	.
$—OC_8H_{17}$	.	49	—	—	. 62	.	71	.	73	.
$—OC_9H_{19}$	.	65	—	—	(. 47)	.	67	.	70	.
$—OC_{10}H_{21}$	.	66	(.	45)	. 68	.	70	.	72	.
$—OC_{11}H_{23}$	.	77	(.	44	. 65)	—	—	—	—	
$—OC_{12}H_{25}$	.	63	(.	42)	. 69	—	—	—	—	.
$—OC_5H_{11}$ [a)]	.	77	—	—	—	—	—	—	—	.
$—OCH_2CH{=}CH_2$	.	42	—	—	(. 40)	.	55	—	—	.
$—C_8H_{17}$	.	33	—	—	(. 23)	—	—	—	—	.
$—C_{12}H_{25}$	.	41	—	—	(. 39)	—	—	—	—	.

[a] (S)-2-methyl-butyl

TABLE V

(S)-4-n-alkyloxyphenyl-4-(2-chloro-3-methyl-butanoyloxy)-benzoates

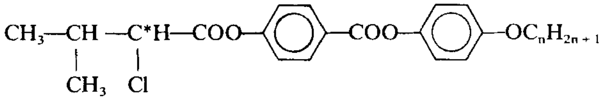

No.	n	Cr		N*		is
5/1	6	.	52	(.	50)	.
5/2	8	.	60	(.	51)	.
5/3	9	.	65	(.	48)	.

contain impurities which lead to intervals in the phase transition temperatures. Especially the optical purity of the compounds could not be investigated. Comparisons with the transition temperatures of corresponding racemic compounds lead to the conclusion that depending on the synthesis conditions certain amounts of racemate may be present in some of the listed compounds.

The classification of the phases was made according to the results of texture observation. The smectic G phase of the compound 1/10 showed a mosaic texture without homeotropic regions. The smectic B phases of the compounds in Table II exhibit mosaic textures with homeotropic domains. Several compounds which are cholesteric have additional blue phases. Only in Table IV the corresponding transition temperatures are given where the existence regions of the blue phases in the respective compounds are unusually broad.

TABLE VI

(S)-4-(4-n-alkyloxy-benzoyloxy)-phenyl-4-(2-chloro-3-methyl-butanoyloxy)-benzoates

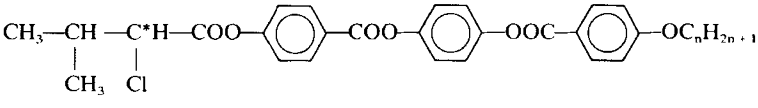

No.	n	Cr		C*		N*		is
6/1	6	.	90	.	95	·	208	.
6/2	7	.	95	.	100	.	191	.
6/3	8	.	94	.	108	.	189	.
6/4	9	.	106	.	110	.	190	.
6/5	10	.	99	.	123	.	193	.

TABLE VII

(S)-4-(2-chloro-3-methyl-butanoyloxy)-benzoates

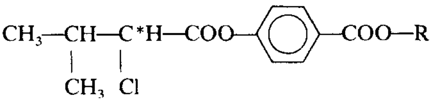

No.	R	Cr		C*		N*		is
	—H	.	138	—	—	—	—	.
7/1	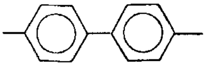	.	83	—	—	—	—	.
7/2	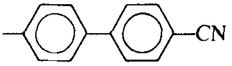	.	114	—	—	.	188	.
7/3	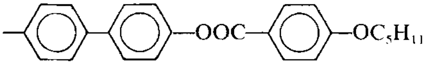	.	180	.	202		340	.
7/4	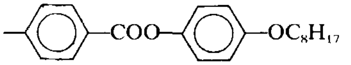	.	85		107	.	182	.

The chiral starting products for the synthesis are: valine (Tables I–VII, XII, XIII), leucine (Tables VIII, IX) and isoleucine (Tables X, XI).

As can be seen from the Tables I, III, VI, VII, VIII and X, many of the three ring compounds exhibit C* phases with relatively high transition temperatures. Two ring compounds as given in Tables IV, IX and XI have C* phases with much lower transition temperatures, thus they are useful as low melting mixture components.

Table XIV presents some known compounds which were used as mixture components.

TABLE VIII

(S)-4-(2-chloro-4-methyl-pentanoyloxy)-4′-(4-n-alkyloxy-benzoyloxy)-biphenyls

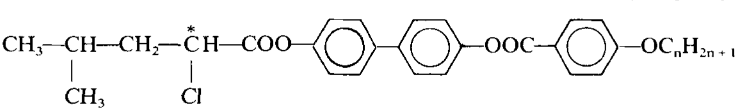

No.	n	Cr		C*		A		N*		is
8/1	5	.	100	.	116	—	—	.	158	.
8/2	6	.	86	.	122	.	142	.	156	.
8/3	7	.	81	.	132	.	145	.	160	.
8/4	8	.	80	.	137	.	154	.	160	.

TABLE IX

(S)-1-(2-chloro-4-methyl-pentanoyloxy)-4-(4-n-alkyloxy-benzoyloxy)-benzenes

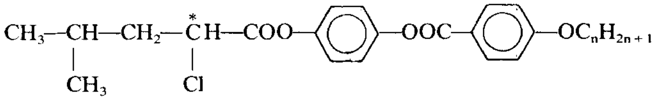

No.	n	Cr		C*		A		is
9/1	8	.	59	—	—	(.	54)	.
9/2	9	.	59	(.	30	.	52)	.
9/3	10	.	47	(.	36)	.	54	.
9/4	11	.	59	—	—	.	54	.

TABLE X

(S)-4-(2-chloro-3-methyl-pentanoyloxy)-4′-(4-n-alkyloxy-benzoyloxy)-biphenyls

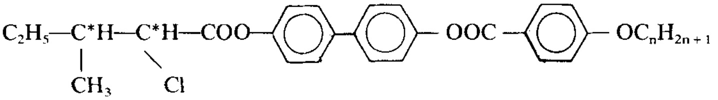

No.	n	Cr		C*		N*		is
10/1	8	.	90	.	177	.	195	.
10/2	12	.	90	.	159	.	190	.

TABLE XI

(S)-1-(2-chloro-3-methyl-pentanoyloxy)-4-(4-n-alkyloxy-benzoyl)-benzene

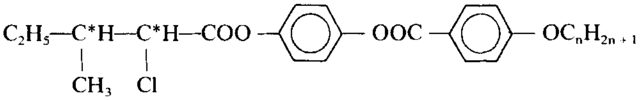

No.	n	Cr		C*		A		N*		is
11/1	6	.	64	—	—	(.	42	.	45)	.
11/2	7	.	62	—	—	(.	33	.	38)	.
11/3	8	.	72	(.	20	.	48	.	49)	.
11/4	9	.	63	—	—	(.	52)	—	—	.
11/5	11	.	72	—	—	(.	57)	—	—	.

TABLE XII

(S)-5-n-Alkyl-2-(4-(2-chloro-3-methyl-butanoyloxy)-phenyl)-pyrimidines

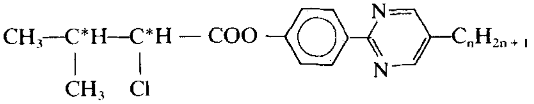

No	n	Cr		is
12/1	7	.	60	.
12/2	9	.	45	.

TABLE XIII

(S)-5-n-Alkyl-2-(4-(4-(2-chloro-3-methyl-butanoyloxy)-benzoyloxy)-phenyl)-pyrimidines

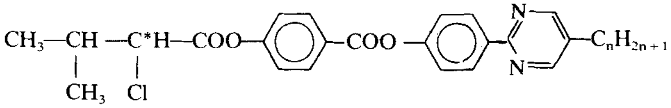

No	n	Cr		C*		N*		is
13/1	6	.	85	—	—	.	149	.
13/2	7	.	70	.	96	.	202	.
13/3	9	.	62	(.	69)	.	157	.

TABLE XIV

		Reference
14/1	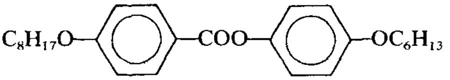	2a)
14/2	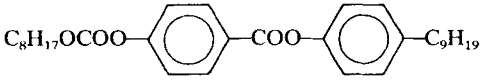	2b)
14/3	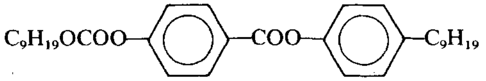	2b)

MIXTURES

In the following we present some two- and multicomponent mixtures exhibiting C* phases in a low-temperature region. In some mixtures also non-chiral compounds are included. In most cases the C* phases can be supercooled to temperatures well below the melting points.

Two component mixtures

Component	Mole %	Mixture no	Phase transitions
4/6	50	(1)	cr 30C* 43 A 70 N* 72 is
4/8	50		
4/6	65	(2)	cr 28C* 72 A 94 N* 109 is
1/6	35		

Three component mixtures

Component	Mole %	Mixture no	Phase transitions
4/4	35	(3)	cr 19 C* 49 A 79 N* 93 is
4/6	37.5		
1/6	27.5		
4/6	67.5	(4)	cr 28 C* 62 A 78 N* 99 is
1/6	22.5		
14/1	10		
1/6	16.1	(4 b)	(cf Figure 3)
4/6	48.2		
C8	35.1		

Four component mixtures

4/4	45	(5)	cr 16 C* 43 A 61 N* 68 is
4/8	15		
14/1	16		
14/3	24		
4/4	44	(6)	cr 17 C* 53 A 70 N* 90 is
1/6	21		
14/1	14		
14/2	21		

Five component mixtures

4/4	17	(7)	cr 18 C* 56 A 76 N* 88 is
4/6	19		
1/6	14		
14/1	20		
14/2	30		

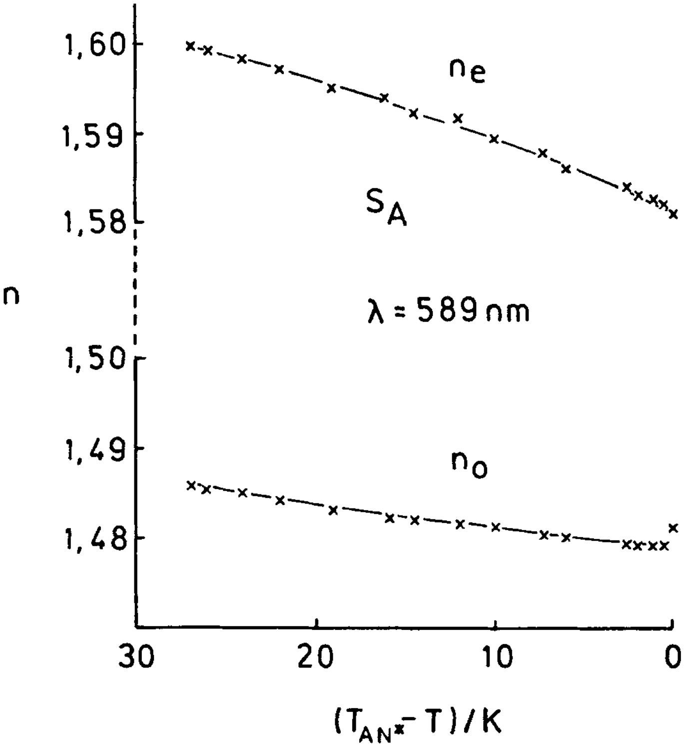

FIGURE 4 Refractive indices as a function of temperature in the smectic A phase of binary mixture no. 1.

MELTING ENTHALPIES

Melting enthalpies are useful for calculation of eutectic mixtures or the solubility of single components in mixtures.

Melting enthalpies have been determined by means of a Perkin-Elmer differential scanning calorimeter DSC 2.

Compound no	$\Delta_F H$/kJ · mol^{-1}
4/4	40.1
4/5	45
4/6	42
4/8	48
1/6	23
1/9	48

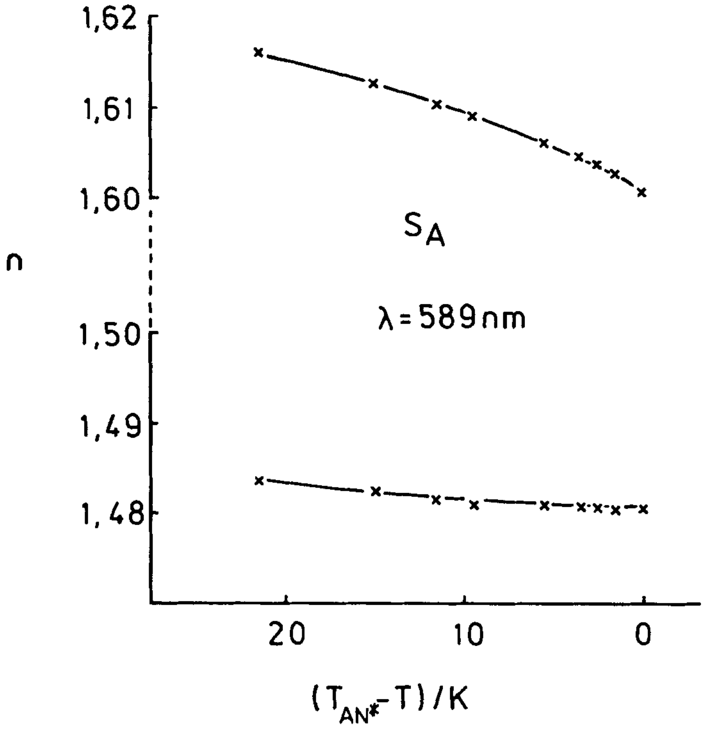

FIGURE 5 Refractive indices as a function of temperature in the smectic A phase of binary mixture no. 2.

REFRACTIVE INDICES

The refractive indices of the smectic A phase were measured by Abbe's double prism method.[4] The measurements were made in monochromatic light of wavelength 589 nm. The following mixtures were investigated.

Binary mixture no 1

4/6	50 mol %
4/8	50 mol %

Binary mixture no 2

4/6	65 mol %
1/6	35 mol %

As can be seen from the figures, the birefringence has fairly standard magnitude in going from 0.10 to 0.11 and 0.11 to 0.12, respectively for the two mixtures, between the N*-A and the A-C* transition points.

TILT ANGLES (X-RAY VALUES)

Figure 6 displays the results of tilt angle determinations in the C* phase of two materials. The tilt angle α is calculated using the equation

$$\alpha = \cos^{-1}\left(\frac{d_c}{d_A}\right)$$

Here d_A and d_C are the smectic layer spacings in the A and the C* phases, respectively, measured versus temperature in a small-angle X-ray apparatus.

The measurements in the binary mixture could not be extended to any saturation value at lower temperatures because crystallization occurred. It should further be emphasized that in the case of low tilts the results are strongly influenced by the accuracy of the d value determination. An error of ±0.01° in the measurement of the Bragg

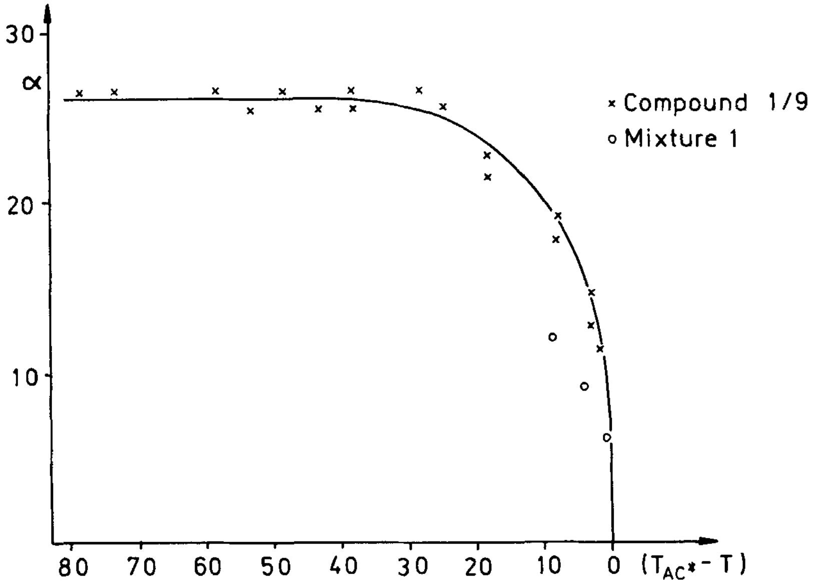

FIGURE 6 Tilt angle as a function of temperature for two materials as determined by X-ray diffraction.

angle leads to an error of ±0.2 Å in our case where $d \simeq 31$ Å. Taking into account the nearly equal values d_A and d_c for tilt angles $\alpha < 10°$, an error of ±3° may result.

ELECTRIC AND ELECTRO-OPTIC MEASUREMENTS

On three of the described substances more extensive physical characterization was carried out, including measurements of spontaneous polarization, tilt angle and optical response times. For the measurements, the liquid crystal sample was prepared between two ITO-coated glass plates that have been given a special electrode pattern by etching in order to have a well-defined overlapping area (in the present case the overlapping area is 16.8 mm^2). The distance between the glass plates was maintained by evaporated silicon-monoxide spacers of 2 μm thickness. The orientation of the smectic layers is such that the layer normal is parallel to the glass plates and the layers are parallel to each other. This orientation is achieved by shearing the plates relative to each other in a specially constructed shear cell as shown in Figure 7. In order to promote a fairly free director at the boundaries and to prevent electric breakthrough in the active area a 1000 Å uniform SiO layer was deposited by normal incidence thermal evaporation. The helix does not have to be unwound by the applied field for the polarization measurements as it would in a thicker sample. It is for some substances, with low polarization and high ionic content, not possible in thick samples to achieve this helix-unwinding because of electrohydrodynamic effects occurring before the necessary field strength is present. In such cases thin cells, with initially unwound helix, is advantageous.

Of great importance, in particular when studying the usually very fast electro-optic switching in ferroelectric liquid crystals, is the resistivity of the conductive ITO-layers on the glass plates since the RC-constant of the integral cell determines the attainable switching times. In the present case, with $R = 535\ \Omega$ and $C = 300$ pF, the integrated electro-optic evaluation system exhibits a limit around 100 ns for the measureable rise and decay times. The shear orientation cell is mounted in a Mettler FP52 hot stage for temperature control and is put on a Zeiss Photomicroscope table for observation under crossed polarizers. The sample temperature is independently measured by a Pt100 resistor element drilled into the sample cell itself. The bridge circuit used is shown in Figure 8. The basic principle is to balance out all purely dielectric contributions to the measured

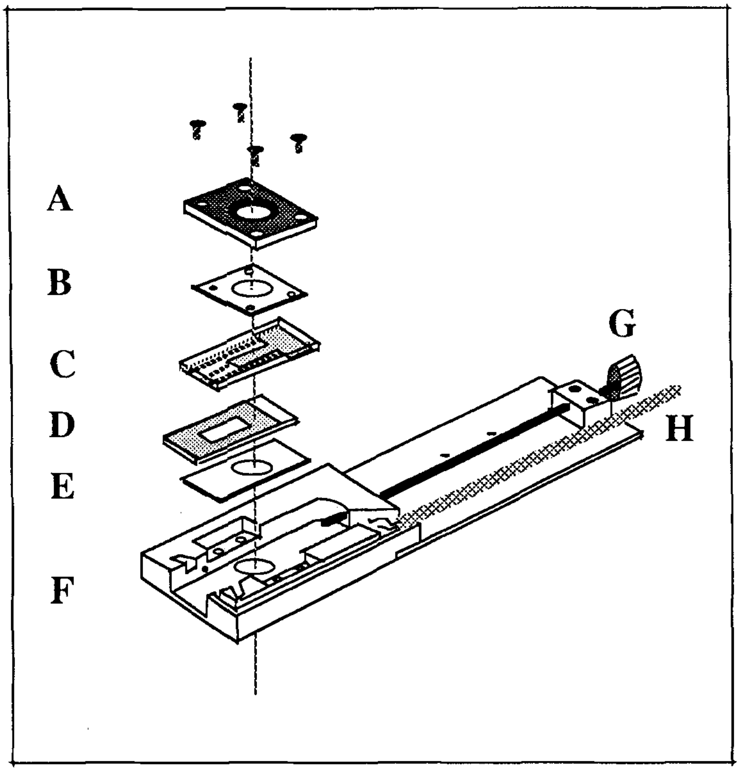

FIGURE 7 Polarization measuring cell. The liquid crystal is between the two glass plates C and D, which are pressed together by the lid A. A silicon rubber E is keeping the plate D in place when shearing, and a teflon sheet B facilitates shearing of the upper plate A. The cell itself F fits into a Mettler FP52 temperature cell, and orientational shear is applied by screw G in the smectic A and C phases. Electric connection is made by grounded coaxial cable H.

current response from the cell, and to retain only the non-linear current from the ferrroelectric dipole switching in the applied sinusoidal driving voltage, this non-linear current resulting in a hysteresis curve.[5]

The bridge is built up from precision electronic parts, and calibrated against a HP 4192A impedance analyzer. For the measurements of spontaneous polarization only C_2 has to be known. If dielectric measurements are also performed all parts C_1, C_2, C_B, R_B, have to be calibrated. The capacitors $C_1 = C_2$ are variable in ten steps from 5 nF to 1 μF and C_B and R_B is continuously variable from 10 nF to 4 pF and 100 Ω to 130 MΩ, which gives a balanced matching with our

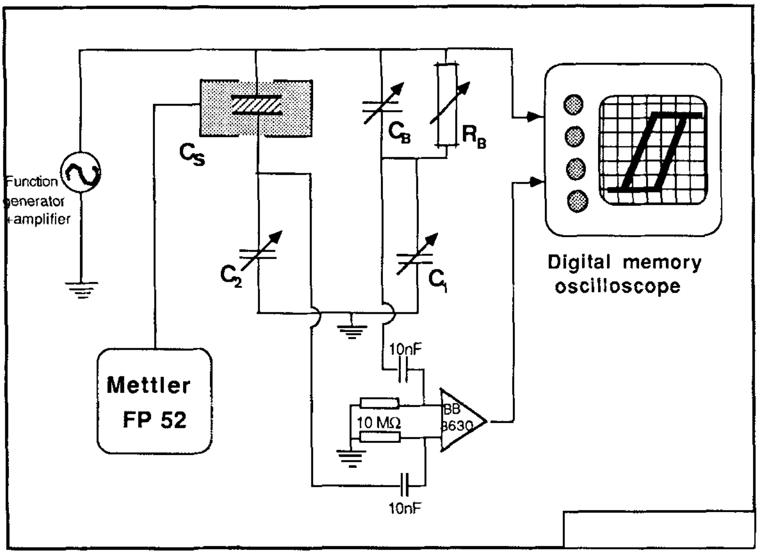

FIGURE 8 Bridge circuit for polarization and dielectric studies of ferroelectric liquid crystals. A high voltage amplifier supports the bridge with 0–130 V AC voltage in the frequency interval 1 Hz—100 kH. The sample cell capacitor C is balanced by component C and R to yield a precisely compensated hysteresis loop.

sample cell (empty capacitance 75 pF) for most of the studied liquid crystal materials. With this bridge it is possible to measure the polarization with a sensitivity of 0.01 nC/cm^2.

A well saturated and distorsion-free hysteresis loop is necessary for accurate measurements. In practice, it turns out that a very disturbing influence is coming from ionic currents in the sample, which in extreme cases can give a hysteresis curve very similar to the ferroelectric one, showing up even in the isotropic phase.

Experimentally, one has to choose a proper driving voltage and frequency where these influences are minimized. This means in general that the component values for compensating resistance and capacitance in the bridge has to be adjusted properly when measuring at different temperatures. For too high measuring field strengths the hysteresis loop will be distorted in a characteristic way due to electrohydrodynamic flow phenomena in the cell.[6]

In Figure 9 is shown a typical hysteresis loop (mixture 4 b) at 30°C. The spontaneous polarization is directly read on the oscilloscope screen from the amplitude of the hysteresis loop.

The vertical scale in this case is 1 div. = 10.4 nC/cm^2, and the horizontal scale in 1 div. = 5V. A symmetric bridge was used (C_1

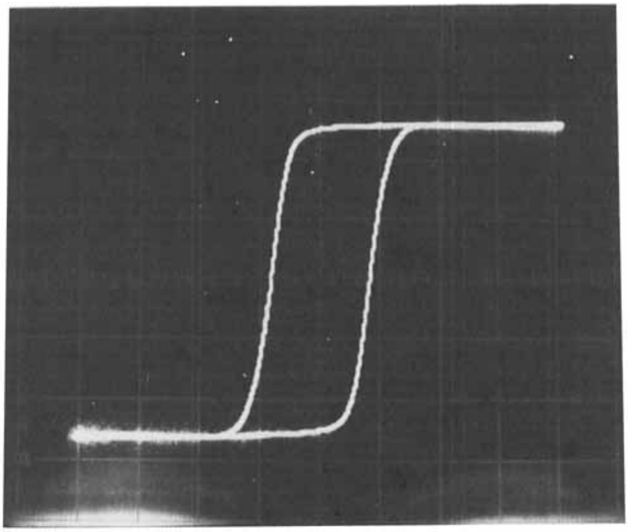

FIGURE 9 Hysteresis loop for mixture 4b (Figure 3) at $T = 30°\mathrm{C}$
Vertical scale: 1 div. = 10.4 nC/cm^2.
Horizontal scale: 1 div. = 5V.

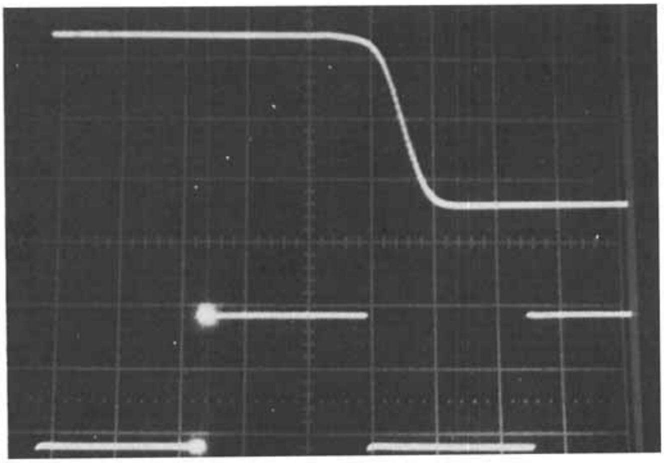

FIGURE 10 Upper curve: Optical response of mixture 4b to square wave voltage. Time base: 50 μs/div.
Lower curve: Driving voltage. Time base: 2μs/div.
Vertical scale: 5 V/div.

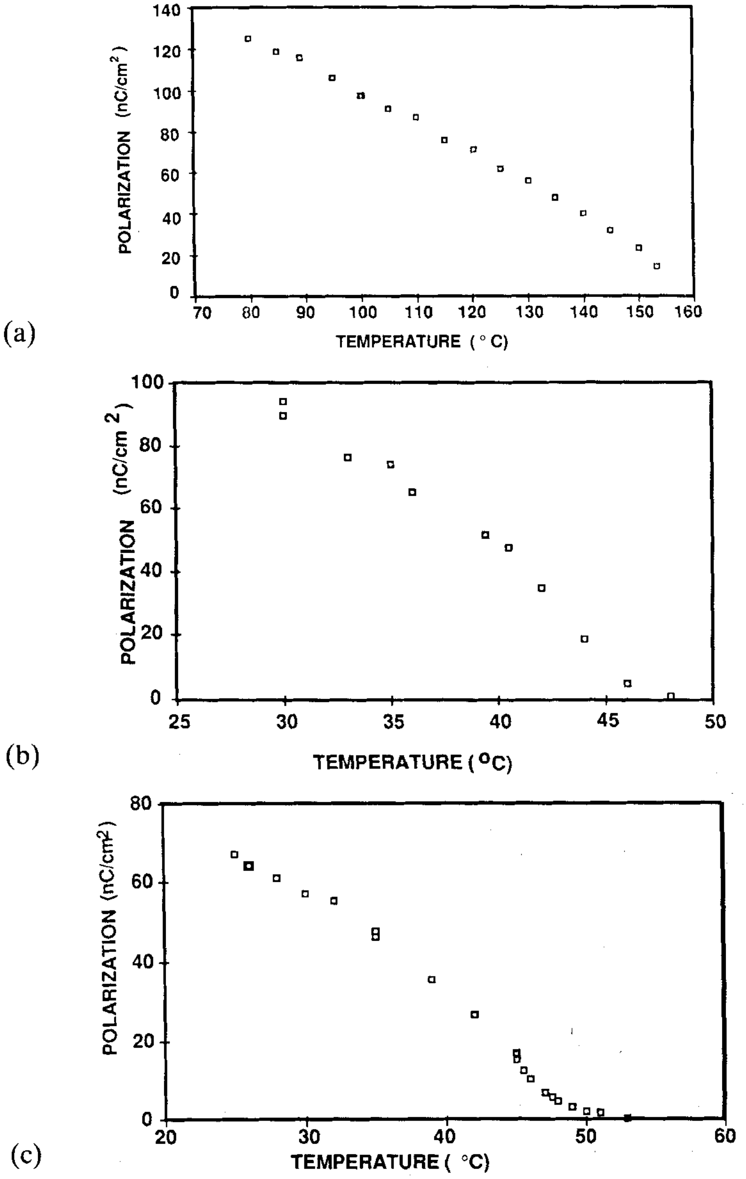

FIGURE 11 Spontaneous polarization as a function of temperature for (a) substance 1/9 (Table I), (b) binary mixture no. 1, (c) mixture 4b. Typical experimental conditions in the three cases:

(a) at 80°C: $U = 42\ V_{pp}$, $f = 1150$ Hz, $R = 0.22$ MΩ, $C = 670$ pF,
(b) at 30°C: $U = 68\ V_{pp}$, $f = 600$ Hz, $R = 18$ MΩ, $C = 365$ pF,
(c) at 28°C: $U = 56\ V_{pp}$, $f = 300$ Hz, $R = 110$ MΩ, $C = 260$ pF.

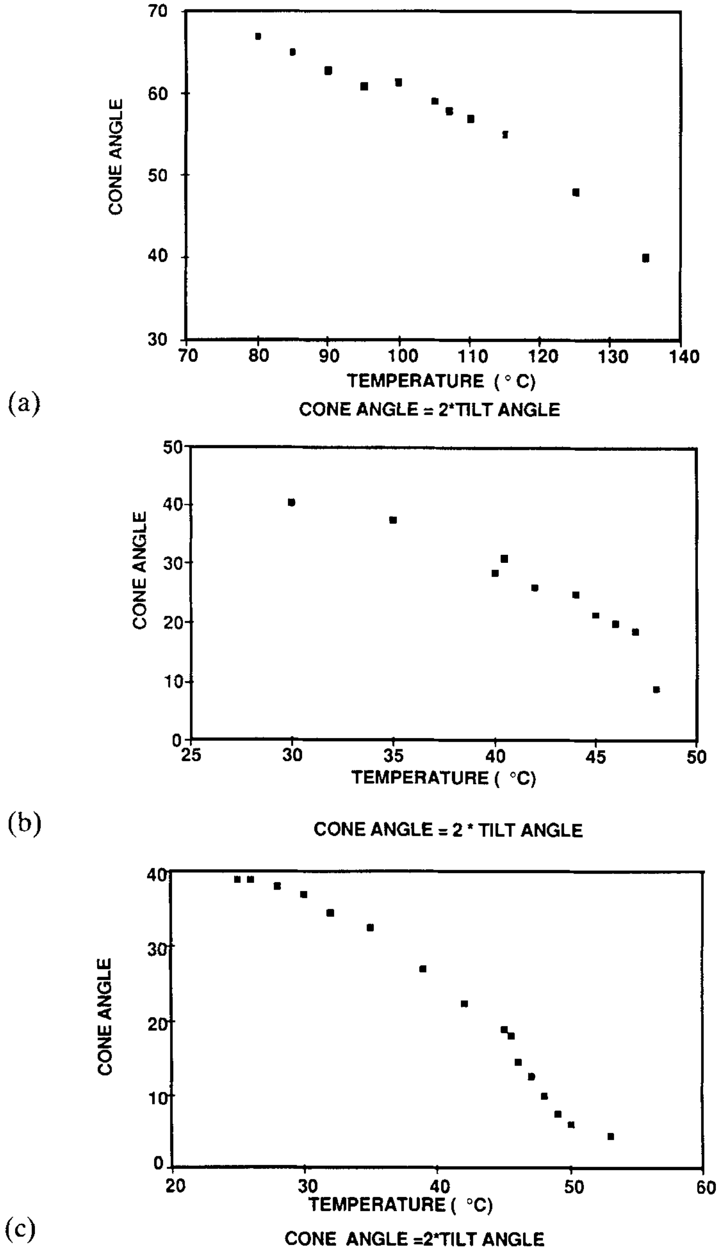

FIGURE 12 Tilt angle as a function of temperature for (a) substance 1/9, (b) binary mixture no. 1, (c) mixture 4b. Note that the full cone angle (which is twice the smectic tilt angle) is displayed.

$= C_2$) with a sine-wave voltage of 20 V amplitude and 300 Hz frequency. If a square-wave voltage is instead applied, we can measure the electro-optic response time τ between 10% and 90% transmission through crossed polarizers. In Figure 10 is shown a typical response curve (mixture 4b). The upper curve is the optical response from a fast photo-diode (time base 50 μs/div.) and the lower curve is the driving voltage (time base 2 μs/div.; vertical scale 5V/div.)

Our results for the spontaneous polarization of the compounds are shown in Figure 11. It is observed experimentally that the behaviour near the phase transition is strongly dependent on the applied field, suggesting that in this region the smectic tilt angle, and thus also the

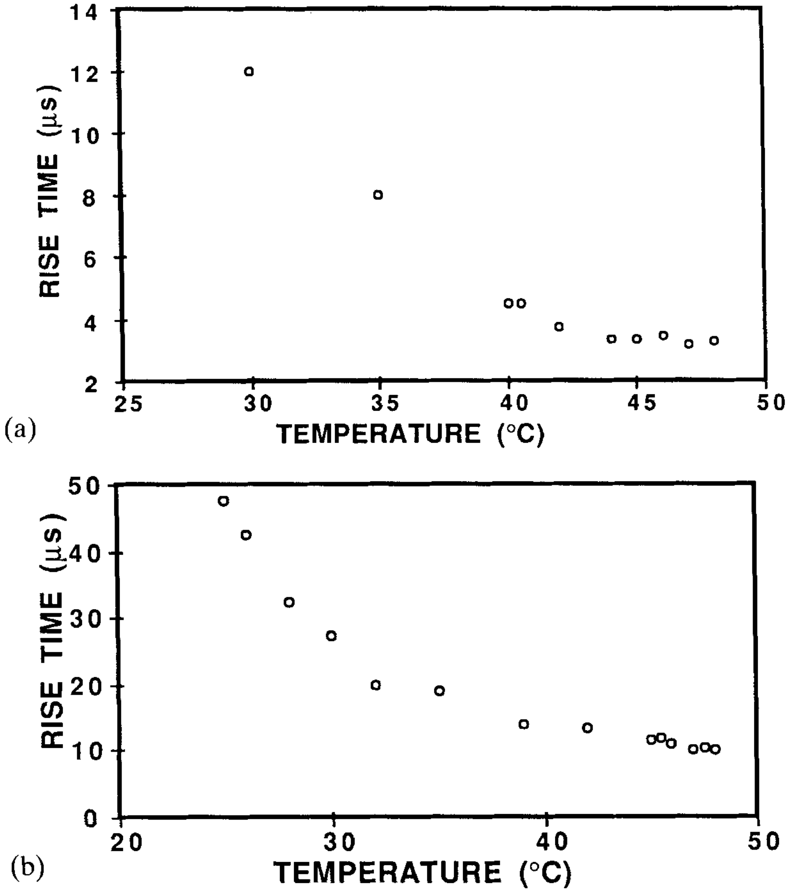

FIGURE 13 Optical rise time versus temperature for (a) binary mixture no. 1, and (b) mixture 4b.

measured value of the spontaneous polarization, is easily changed by the applied field. The sign of the spontaneous polarization, as defined by the relation $P = P_0 \hat{z} \times \hat{n}$, is found to be negative (here $\hat{z}$ is the smectic layer normal and $\hat{n}$ is the director) for all three components. The smectic tilt angle is measured by rotating the well-aligned sample between crossed polarizers to observe the two extreme optic axes orientations corresponding to two different polarities of the applied field. The tilt angle as a function of temperature for the three compounds is shown in Figure 12. We do not here present curve fits for the polarization and tilt angle data, since existing theories for the critical behaviour of these parameters for their evaluation also require input of other physical quantities such as heat capacity and dielectric constant.[7,8] Optical risetime measurements for mixture 4b and binary mixture no. 1 are presented in Figure 13. The low values of the response times, especially for binary mixture no. 1, indicates a low rotational viscosity.

Acknowledgment

This work has been supported by the National Swedish Board of Technical Development under Grant No 84-3691.

References

1. P. Karrer, H. Reschofsky and W. Kaase, *Helv. Chim Acta*, **30**, 271 (1947).
2. D. Demus, H. Demus and H. Zaschke, Flüssige Kristalle in Tabellen, Deutscher Verlag für Grundstoffindustrie Leipzig 2nd edition 1974 a) p. 68, b) p. 73.
3. D. Demus, H. Zaschke, Flüssige Kristalle in Tabellen II, Deutscher Verlag für Grundstoffindustrie, Leipzig 1984.
4. G. Pelzl, H. Sackmann, *Sympos. Faraday Soc.* No. 5, 68 (1971).
5. H. Diamant, K. Drenck and R. Pepinsky, *Rev. Sci. Instr.*, **28**, 30 (1957).
6. S. Kai, T. Hashimoto, K. Ose and M. Imasaki, *Mol. Cryst. Liq. Cryst.*, **130**, 143 (1985).
7. S. Dumrongrattana and C. C. Huang, *Phys. Rev. Lett.*, **56**, 464 (1986).
8. B. Zeks, *Mol. Cryst. Liq. Cryst.*, **114**, 259 (1984).